Force Transmission Evaluation in Spatial Mechanisms with Higher Pairs

Chao Chen* **Jorge Angeles**
chao.chen@mail.mcgill.ca angeles@cim.mcgill.ca
Department of Mechanical Engineering & Centre for Intelligent Machines
McGill University, Quebec, Canda

ABSTRACT

We propose a generalized transmission index for spatial mechanisms, based on the virtual coefficient between the transmission wrench screw and the output twist screw. Compared with other indices, this index is well defined in any case and able to evaluate the force transmission quality more precisely. We apply this index to mechanisms with higher pairs and show that the pressure angle is a special case of our index.

Évaluation de la transmission des forces dans les mécanismes spatiaux à paires cinématiques supérieures

RÉSUMÉ

Nous proposons un indice de transmission gńéralisé pour les mécanismes spatiaux, basé sur le coefficient virtuel entre le torseur de transmission et le visseur cinématique de l'élément entraîné. Le nouvel indice est défini sans ambigüité dans tous les cas et permet d'évaluer la qualité de transmission des forces plus précisément que les indices connus. L'indice est appliqué à des mécanismes comportant de couples cinématiques supérieures, tout en démontrant que l'angle de pression n'est qu'un cas spécial de notre indice.

1 Introduction

In the design of a mechanism for a specific motion transmission, the quality of force transmission is a key issue. The transmission angle was introduced by Alt [1], and developed by Hain [2] for planar linkages, while the pressure angle was proposed by J.V. Poncelet for cam transmissions [3]. However, these indices are not suitable for some novel mechanisms such as elliptical gears, general spatial gears, and speed reducers based on cam-roller-followers [4], as well as some traditional mechanisms such as indexing mechanisms.

*Address all correspondence to this author.

Here, we briefly recall the indices available for spatial mechanisms. The virtual coefficient, introduced by Ball [5], was used as a transmission factor by Yuan, Freudenstein, and Woo for spatial mechanisms [6], the value of this factor varying from $-\infty$ to $+\infty$. Sutherland and Roth introduced the transmission index (TI), a normalized form of the transmission factor [7], which is a mile stone. Nevertheless, the TI is undefined in some cases and not applicable to mechanisms with higher pairs. Moreover, the maximum used to normalize the virtual coefficient is not a constant in general, which may result in the misleading information of the transmission quality. Tsai and Lee developed a new TI, the transmissivity index, which can be defined in any case by constructing a coordinate frame originated at the physical center of the floating joint on the output link [8]. However, the maximum developed here is neither a constant.

We propose here a generalized transmission index (GTI). The GTI is well-defined in any case, able to represent the transmission performance precisely, and applicable to mechanisms with higher pairs. We also derive the applicable range of the pressure angle. Moreover, applications to mechanisms with higher pairs are given.

2 Virtual Coefficient and Reciprocity

In general, a screw can be represented in dual-number form as

$$\hat{\mathbf{s}} = \mathbf{e} + \epsilon\mathbf{m}$$

where the primal part $\mathbf{e}$ is the unit vector in the direction of the screw axis, the dual part $\mathbf{m}$ being the moment of the screw with respect to the origin, while ϵ is the dual unity, which is defined such that

$$\epsilon \neq 0, \qquad \epsilon^2 = 0$$

Considering one arbitrary point Q, of position vector $\mathbf{q}$ on the screw axis, we have

$$\mathbf{m} = \mathbf{q} \times \mathbf{e} + p\mathbf{e} \tag{1}$$

with p defined as the pitch of the screw, namely,

$$p = \mathbf{e}^T\mathbf{m}$$

Given two screws $\hat{\mathbf{s}}_1$ and $\hat{\mathbf{s}}_2$, their dot product is given by

$$\hat{\mathbf{s}}_1^T\hat{\mathbf{s}}_2 = \mathbf{e}_1^T\mathbf{e}_2 + \epsilon(\mathbf{e}_1^T\mathbf{m}_2 + \mathbf{m}_1^T\mathbf{e}_2) \tag{2}$$

The dual part of the right-hand side in eq. (2) is the *virtual coefficient*, $\tilde{\omega}_{12}$, between these two screws [9]. Considering eq. (1) and introducing two points Q_1 and Q_2, of position vectors $\mathbf{q}_1$ and $\mathbf{q}_2$, on each of the two screw axes, correspondingly, the virtual coefficient can be expressed as

$$\begin{aligned}
\tilde{\omega}_{12} &= \mathbf{e}_1^T\mathbf{m}_2 + \mathbf{m}_1^T\mathbf{e}_2 && \text{(3a)}\\
&= (p_1 + p_2)\mathbf{e}_1^T\mathbf{e}_2 + (\mathbf{q}_1 - \mathbf{q}_2)^T(\mathbf{e}_1 \times \mathbf{e}_2) \\
&= (p_1 + p_2)\cos\vartheta - d\sin\vartheta && \text{(3b)}
\end{aligned}$$

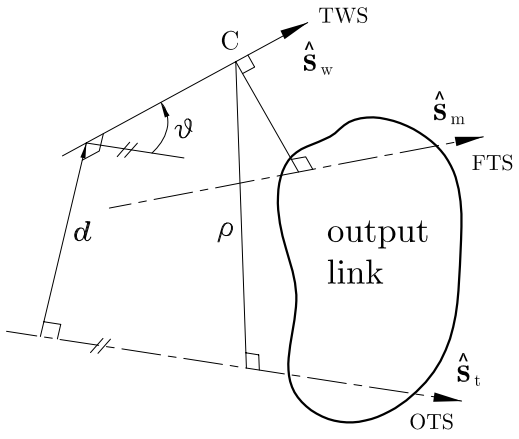

Figure 1: The characteristic point on a spatial output link

where d is the distance from $\hat{\mathbf{s}}_2$ to $\hat{\mathbf{s}}_1$ and ϑ is the angle from $\hat{\mathbf{s}}_2$ to $\hat{\mathbf{s}}_1$ in the direction of a right-handed screw moving along d. Equation (3b) gives a slightly different form of the virtual coefficient when compared with Ball's definition [5], which is one-half that given above. However, this difference does not affect the ensuing derivations.

Considering a wrench represented by $F\hat{\mathbf{s}}_1$ and a twist by $\omega\hat{\mathbf{s}}_2$, the power developed by the wrench on the body moving with the foregoing twist is $F\omega\tilde{\omega}_{12}$. Therefore, the bigger the virtual coefficient, the larger the said power, and the better the force transmission. In other words, a "smaller" wrench is required to transmit the same power to the output link in the presence of a higher virtual coefficient.

When the virtual coefficient vanishes, the two screws are said to be reciprocal to each other, i.e.,

$$\mathbf{e}_1^T\mathbf{m}_2 + \mathbf{m}_1^T\mathbf{e}_2 = 0$$

It is well known that the *constraint wrench* acting on a floating lower pair is reciprocal to the *feasible twist* allowed by this pair [5].

3 Transmission Index

3.1 Transmission Wrench Screw and Transmission Index

The prime function of mechanisms is to transmit motion from the input joint to the output joint. As a result, the load applied at the output joint is transmitted to the input joint. The internal wrench arising because of the transmission is called the *transmission wrench*. Since the magnitude of the load is not necessary to evaluate the quality of a transmission, we focus only on the *transmission wrench screw* (TWS).

According to eq. (3), the virtual coefficient between a TWS $\hat{\mathbf{s}}_w$ and an *output twist screw* (OTS) $\hat{\mathbf{s}}_t$ is given by

$$\tilde{\omega}_{wt} = (p_w + p_t)\cos\vartheta - d\sin\vartheta \tag{4}$$

where p_w and p_t are the pitches of $\hat{\mathbf{s}}_w$ and $\hat{\mathbf{s}}_t$, respectively, while d is the distance from $\hat{\mathbf{s}}_t$ to

$\hat{\mathbf{s}}_w$ and ϑ is the angle from $\hat{\mathbf{s}}_t$ to $\hat{\mathbf{s}}_w$ in the direction of a right-handed screw moving along d, as illustrated in Fig. 1

In order to obtain a finite, dimensionless index, the TI was defined in [7] as

$$TI = \frac{|\tilde{\omega}_{wt}|}{|\tilde{\omega}_{wt}|_{max}}$$

Both the transmissivity proposed in [8] and the GTI developed here follow this definition. The only differences among the three indices lies in the definition of the maximum value of the virtual coefficient.

3.2 Characteristic Point and Maximum Virtual Coefficient

Sutherland and Roth introduced the *characteristic point* to find the putative maximum value of the virtual coefficient. This point is defined as the point C on the TWS axis closest to the axis of the *feasible twist screw* (FTS) $\hat{\mathbf{s}}_m$ of the floating joint on the output link, as shown in Fig. 1 [7]. In consequence, the characteristic length ρ was defined as the distance from the characteristic point to the OTS. Among all possible TWSs with a constant pitch p_w and passing through C for a given OTS, the maximum virtual coefficient is given by

$$|\tilde{\omega}_{wt}|_{max} = \sqrt{(p_w + p_t)^2 + \rho^2} \tag{5}$$

where p_w and p_t are the pitches of the TWS and the OTS, respectively, and ρ is the characteristic length.

However, the definition of the characteristic point encounters some problems: (1) it is undefined if the axes of the TWS and the FTS are parallel; (2) the axis of the FTS of the floating joint is not defined if the joint is prismatic (P), spherical (S) or planar (F); and (3) this definition cannot be applied to a floating higher pair. Furthermore, since p_w and ρ are not constant in general, the TI cannot match the virtual coefficient.

In trying to solve the above problems, Tsai and Lee defined the transmissivity, by defining the maximum of the virtual coefficient as [8]

$$|\tilde{\omega}_{wt}|_{max} = \|\mathbf{e}_w\|\|\mathbf{m}_t\| + \|\mathbf{m}_w\|\|\mathbf{e}_t\| = \|\mathbf{m}_t\| + \|\mathbf{m}_w\| \tag{6}$$

where $\mathbf{e}_w$ and $\mathbf{e}_t$ are unit vectors. The moments are computed with respect to the physical center of the floating joint on the output link. Nevertheless, the maximum given by eq. (6) is still local, so that the transmissivity cannot match the virtual coefficient.

Here, we give our definition based on the maximum given by eq. (5). Before doing this, we describe the roles of the characteristic point C and length ρ defined by Sutherland and Roth.

According to eq. (4), we have

$$\begin{aligned}
\tilde{\omega}_{wt} &= \sqrt{(p_w + p_t)^2 + d^2}(\cos\alpha\cos\vartheta - \sin\alpha\sin\vartheta) \\
&= \sqrt{(p_w + p_t)^2 + d^2}\cos(\alpha + \vartheta) \\
&\leq \sqrt{(p_w + p_t)^2 + d^2}
\end{aligned} \tag{7}$$

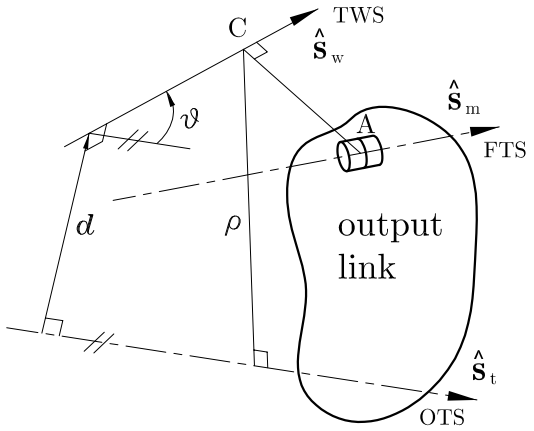

Figure 2: The characteristic point on a spatial output link

where

$$\cos\alpha = \frac{p_w + p_t}{\sqrt{(p_w + p_t)^2 + d^2}} \qquad \sin\alpha = \frac{d}{\sqrt{(p_w + p_t)^2 + d^2}}$$

Comparing eq. (7) with eq. (5), we must have $|d| < \rho$. Since $|d|$ measures the distance between the axes of the TWS and the OTS, it is reasonable to define ρ as the distance between the OTS axis and a point on the TWS axis, which is the characteristic point C. Notice that ρ is a length characterizing the size of the mechanism at hand. On the other hand, the output link is physically connected to the output joint (the OTS) and bears the load directly. Hence, ρ can simply characterize the length of the output link. For this purpose, the point C must be chosen as the point on the TWS axis closest to the *physical floating joint* on the output link.

By representing the floating joint on the output link as a screw, Sutherland and Roth encountered the problems we have mentioned. Moreover, Sutherland and Roth's characteristic length may be far from the actual size of a mechanism, and hence, may yield an unreasonable TI. Therefore, we apply the *point representation* of the floating joint here; the floating joint on the output link is represented as the *point of application* A of the wrench transmitted, as shown in Fig. 2; this point is defined as the centroid of the contact region in the physical joint. More specifically, the point A of a R, H or C joint is the mid-point of the contact line segment on its axis; for a S joint, the point A is the sphere center; for a P or F joint, the point A is the geometric center of the physical contact area.

Then, we define the characteristic point as the point on the TWS closest to point A. Consequently, the characteristic point and the characteristic length ρ are uniquely defined, even if the two axes of the TWS and the FTS are parallel, or the floating joint is a P, S, F, or a higher pair. Similar to eq. (5), we define the global maximum as

$$|\tilde{\omega}_{wt}|_{max} = \max_x \{\sqrt{(p_w + p_t)^2 + \rho^2}\}$$

where x is the output displacement, i.e., the output rotation angle if the output joint is R or

H; or the output translation length if the output joint is P. Therefore, the GTI is given by

$$\mathrm{GTI} = \frac{|(p_w + p_t)\cos\vartheta - d\sin\vartheta|}{\max_x\{\sqrt{(p_w + p_t)^2 + \rho^2}\}} \tag{8}$$

which can match the virtual coefficient exactly.

If one of the pitches of the TWS and the OTS is infinite, we have

$$\begin{aligned}\mathrm{GTI} &= \lim_{p_t \text{ or } p_w \to \infty} \frac{|(p_w + p_t)\cos\vartheta - d\sin\vartheta|}{\max_x\{\sqrt{(p_w + p_t)^2 + \rho^2}\}} \\ &= |\cos\mu|\end{aligned}$$

Furthermore, we have

Theorem 3.1 *The virtual coefficient and the GTI vanish if the pitches of both the TWS and the OTS are infinite.*

The physical meaning of the theorem is apparent: A moment develops zero power on a rigid body undergoing a pure translation. Hence, the GTI vanishes.

4 GTI for Mechanisms with Higher Pairs

Since a higher pair usually can transmit only pushing force, the TWS degenerates into the *transmission force line* (TFL), which implies $p_w = 0$. By removing the absolute value of the numerator in eq. (8), we have

$$\mathrm{GTI} = \frac{p_t\cos\vartheta - d\sin\vartheta}{\sqrt{p_t^2 + \rho_{max}^2}}$$

Hence, the GTI varies from -1 to $+1$ and can indicate whether the TFL delivers positive or negative power.

According to our definition, the characteristic point C is coincident with the point of application A in a higher pair on the output link. More precisely, A is the mid-point of the contact line segment of the higher pair.

4.1 GTI and Pressure Angle

The pressure angle μ is defined as the angle between the direction of the transmission force and the direction of the velocity of the contact point, as pertaining to the driven element [4, 10]. We now show that the pressure angle is a special case of the GTI and provide the applicable range of the pressure angle.

If the output joint is a revolute pair, as shown in Fig. 3(a), p_t vanishes. Hence,

$$\mathrm{GTI} = \frac{-d\sin\vartheta}{\rho_{max}} = \frac{\rho\cos\mu}{\rho_{max}} \tag{9}$$

the GTI becoming $\cos\mu$ when ρ is constant.

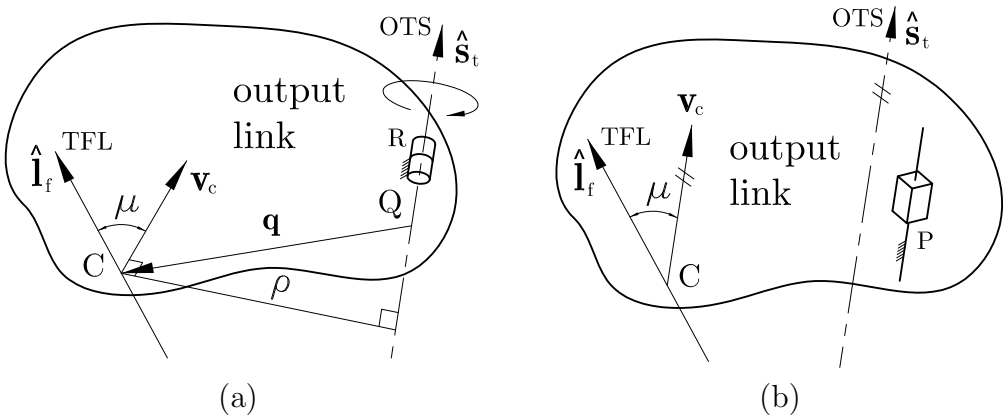

Figure 3: The transmission force line with respect to (a) a revolute output joint; (b) a prismatic output joint

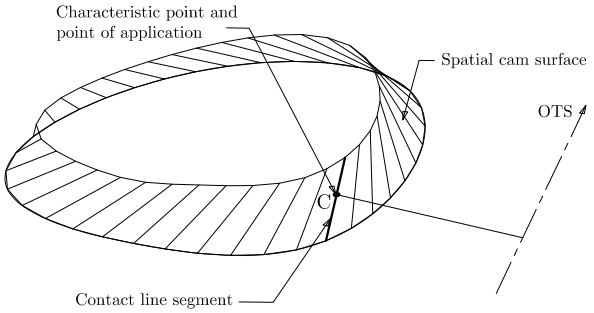

Figure 4: The characteristic point on a spatial cam transmission

If the output joint is prismatic, as shown in Fig. 3(b), then $p_t \to \infty$, i.e.,

$$\mathrm{GTI} = \lim_{p_t \to \infty} \frac{p_t \cos\mu - d \sin\mu}{\sqrt{p_t^2 + \rho_{max}^2}} = \cos\mu$$

If the output joint is a screw pair, then the GTI is no longer proportional to $\cos\mu$. Therefore, the pressure angle is applicable to a mechanism with a higher pair only if (*i*) the output joint is prismatic, or (*ii*) it is revolute and the characteristic length is constant.

We will illustrate the application of the GTI in some typical mechanisms with a revolute output joint, by application of eq. (9).

4.2 Cam-Follower Mechanisms

Since the cam-follower coupling is a higher pair, pertaining to the output link in this three-link mechanism, the characteristic point C is the mid-point of the contact line segment, as shown in Fig. 4, where the follower is ignored. The transmission force line at point C is determined by the contact surface, and hence, the GTI can be readily obtained by eq. (9).

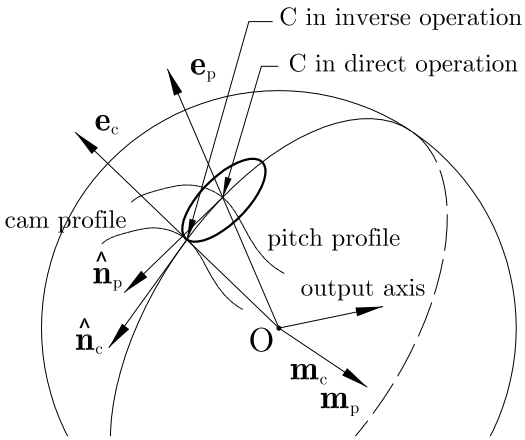

Figure 5: The pitch and contact profiles on a unit sphere

4.3 Cam-Roller-Follower Mechanisms

Although general spatial cam-roller-follower mechanisms are synthesized in [11], the axially symmetric, hyperbolic roller must be coupled via a C pair onto the follower in general. Hence, such mechanism is not practical because a C pair cannot bear any axial load while the cone contact surface between the cam and the roller yields axial force component. Only spherical and planar mechanisms do not require rollers translating along their axes during transmission, and hence, C pairs are replaced with R pairs in their cases.

4.3.1 Planar Case

There are two operations: the direct operation and the inverse operation. In the former, the cam drives the roller-follower; in the latter, the roller-follower drives the cam. Therefore, the characteristic point C in direct operation is the pitch point, the center of the roller according to its definition, while the point C in inverse operation is the contact point on the cam.

The transmission force line can be determined equivalently by either the pitch profile of the cam at the pitch point or the cam profile at the contact point. Then, the GTI will be computed by eq. (9).

4.3.2 Spherical Case

We describe the motion of a spherical mechanism as occurring on the unit sphere. The characteristic point C in direct operation is the pitch point of the cam, i.e., the intersection point between the roller-bearing axis and the unit sphere, while the point C in inverse operation is the contact point of the cam, the intersection point between the contact line and the unit sphere.

The transmission force line $\hat{\mathbf{n}}_c$ is determined by the cam profile at the contact point, as shown in Fig. 5. However, engineers use the pitch profile of the cam to compute the transmission force line $\hat{\mathbf{n}}_p$ because the pitch profile is simpler to manipulate than the cam profile [11]. Although the transmission force lines obtained using the two profiles are different, we have the theorem below.

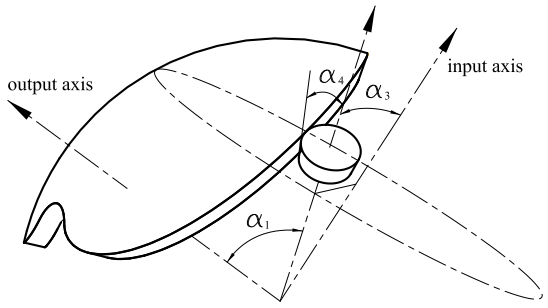

Figure 6: A spherical cam-roller-follower mechanism

Theorem 4.1 *The virtual coefficient between the OTS and the unit normal to the pitch profile and the one between the OTS and the unit normal to the cam profile are the same, when describing the motion of a spherical mechanism on the unit sphere.*

Proof: Let us set the center of a spherical mechanism as the reference point. We have

$$\mathbf{m}_t = \mathbf{0}$$

According to eq. (3a), the virtual coefficient between the TWS and OTS is given by

$$\tilde{\omega}_{wt} = \mathbf{e}_t^T \mathbf{m}_w \tag{10}$$

Notice that the unit normal to the cam profile and the unit normal to the pitch profile are tangent to the same great circle, as shown in Fig. 5. Therefore, both normals yield the same moment, $\hat{\mathbf{m}}_c$ or $\hat{\mathbf{m}}_p$ with respect to the reference point. According to eq. (10), the virtual coefficients obtained by the two unit normals are the same.

4.4 Gear Mechanisms

Although gear pairs are special cases of cam-follower pairs, they are usually studied as friction wheels. Therefore, we choose the mid-point of the pitch line segment in a gear pair as the characteristic point. Determining the TFL by the profile of the tooth, we can readily obtain the GTI from eq. (9).

5 Example: A Spherical Cam-Roller-Follower Mechanism

A spherical cam-follower mechanism is shown in Fig. 6, with design parameters given below:

$$\alpha_1 = 90^\circ; \quad \alpha_3 = 70^\circ; \quad \alpha_4 = 8^\circ; \quad N = 3$$

where α_1 is the angle between the axes of rotation of the cam and the follower; α_3 is the angle between the axes of the follower and the roller; α_4 is the half angle of the cone surface of the roller; and N is the number of rollers on the follower.

The cam profile is given by [4]

$$\mathbf{e}_c = [\,-\tilde{h}_1, -\tilde{h}_2, \tilde{k}_1\,]^T$$

where

$$\begin{aligned}
\tilde{h}_1 &= \tilde{k}_3 \sin\psi - \sin\eta \sin\delta \cos\psi \\
\tilde{h}_2 &= \tilde{k}_3 \cos\psi + \sin\eta \sin\delta \sin\psi \\
\tilde{k}_1 &= \cos\vartheta_2 \cos(\eta) - \sin\vartheta_2 \sin\eta \cos\delta \\
\tilde{k}_3 &= \sin\vartheta_2 \cos\eta + \cos\vartheta_2 \sin\eta \cos\delta \\
\eta &= \vartheta_3 - \alpha_4 \\
\vartheta_3 &= \arctan \frac{\sqrt{A_1^2 + A_2^2}}{B_1} \\
\delta &= \arctan \frac{A_3}{B_2} \\
A_1 &= \cos(\alpha_1 - \vartheta_2) \cos\phi \sin\alpha_3 + \cos\alpha_3 \sin(\alpha_1 - \vartheta_2) \\
A_2 &= \sin\alpha_3 \sin\phi \\
B_1 &= \cos\alpha_3 \cos(\alpha_1 - \vartheta_2) - \cos\phi \sin\alpha_3 \sin(\alpha_1 - \vartheta_2) \\
A_3 &= \sin\alpha_3 \sin\phi \\
B_2 &= \sin\alpha_3 \cos(\alpha_1 - \vartheta_2) \cos\phi + \cos\alpha_3 \sin(\alpha_1 - \vartheta_2) \\
\vartheta_2 &= \arctan \frac{\phi' \sin\alpha_1}{\phi' \cos\alpha_1 - 1} \\
h_1 &= k_3 \sin\psi - \sin\alpha_3 \sin\phi \cos\psi \\
h_2 &= k_3 \cos\psi + \sin\alpha_3 \sin\phi \sin\psi \\
k_1 &= \cos\alpha_1 \cos\alpha_3 - \sin\alpha_1 \sin\alpha_3 \cos\phi \\
k_3 &= \sin\alpha_1 \cos\alpha_3 + \cos\alpha_1 \sin\alpha_3 \cos\phi \\
\phi &= -\pi(1 - 1/N) - \psi/N
\end{aligned}$$

with ψ and ϕ being the input and output angles, respectively.

Although Sutherland and Roth did not define the characteristic point for a mechanisms with a higher pair, we can use our characteristic point to compute the TI. Here, we consider the inverse case. The virtual coefficient is displayed in Fig. 7(a), its maximums defined in [7], [8] and this paper shown in Fig. 7(b). Obviously, only the maximum defined here is a constant. The GTI, Sutherland and Roth's TI, and Tsai and Lee's transmissivity are displayed in Fig. 8, where the TI and the transmissivity are symmetric. Notice that only the GTI matches the virtual coefficient exactly.

6 Conclusions

We proposed the GTI for spatial mechanisms, which is well-defined in any case. The GTI for spatial mechanisms with higher pairs varies from -1 to $+1$, which indicates whether the TFL

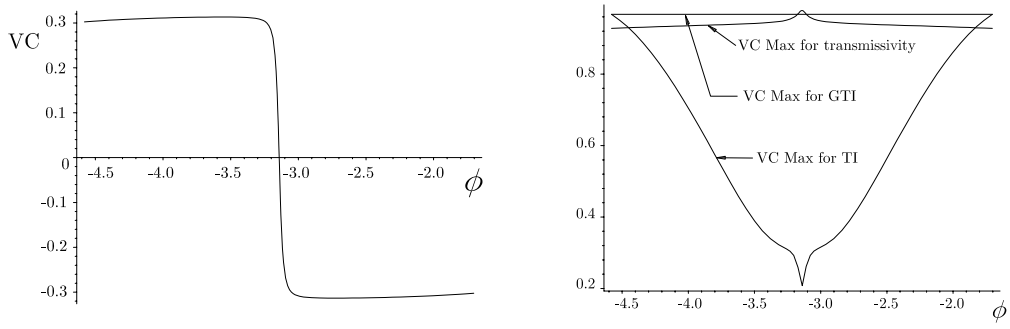

(a) (b)

Figure 7: (a) the virtual coefficient; and (b) the maximum of the virtual coefficient of the GTI, the TI and the transmissivity in the inverse operation of the spherical cam and roller-follower mechanism

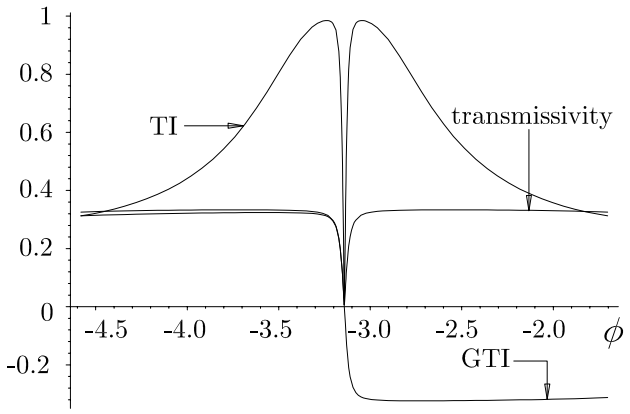

Figure 8: The TI, the GTI and the transmissivity in the inverse operation of the spherical cam and roller-follower mechanism

delivers positive or negative power. We also derived the applicable range of the the pressure angle in a mechanism with a higher pair. Furthermore, by applying dual-number algebra, the virtual coefficient can be formulated concisely, its computation being straightforward.

Acknowledgment

The research work reported here was supported by NSERC (Science and Engineering Research Canada) under Strategic Project No. STP0192750 and FQRNT (Fonds de Recherche sur la Nature et les Technologies).

References

[1] Alt, H., "Der Übertragungswinkel und seine Bedeutung für das Konstruieren periodischer Getriebe", *Werkstattstechnik* 26, 61-64 (1932).

[2] Hain, K., *Applied Kinematics*, MeGraw-Hill, 1967.

[3] Müller, J., "The History of Cams and Cam Mechanisms", *Proc. the 7th World Congress of TMM*, 3, 1649-1652 (1987).

[4] González-Palacios, M. A. and Angeles, J., "The generation of contact surfaces of indexing cam mechanisms. A unified approach", *ASME Journal of Mechanical Design*, 116(2), 369-374 (1994).

[5] Ball, Sir R. S., *A Treatise on the Theory of Screws*, Cambridge University Press, 1900.

[6] Yuan, M. S. C., Freudenstwin, F. and Woo, L. S., "Kinematic Analysis of Spatial Mechanism by Means of Scre Coordinates. Part2–Analysis of Spatial Mechanisms," *Journal of Engineering for Industry, Trans. ASME*, Series B, 91(1), 67-73 (1971).

[7] Sutherland, G. and Roth, B., "A Transmission Index for Spatial Mechanisms", *Journal of Engineering for Industry*, 589-597 (1973).

[8] Tsai, M.J. and Lee, H.W., "The Transmissivity and Manipulability of Spatial Mechanisms", *ASME Journal of Mechanical Design*, 116, 137-143 (1994).

[9] Woo, L. and Freudenstein, F. "Application of Line Geometry to Theoretical Kinematics and the Kinematic Analysis of Mechanical Systems", *Journal of Mechanisms*, Vol. 5, 1970, pp. 417-460.

[10] Jones, J.R., "Mechanisms Pressure Angles and Forces in Cams", *Engineering*, 218, 703-706 (1978).

[11] González-Palacios, M.A. and Angeles, J., *Cam Synthesis*, Kluwer Academic Publishers, 1993.